Angewandte Chemie
Eine Zeitschrift der Gesellschaft Deutscher Chemiker

Supporting Information

A Methyl-TROSY-Based ^{1}H Relaxation Dispersion Experiment for Studies of Conformational Exchange in High Molecular Weight Proteins

Tairan Yuwen, Rui Huang, Pramodh Vallurupalli,* and Lewis E. Kay**

anie_201900241_sm_miscellaneous_information.pdf

Supporting Information

Table of Contents

Materials and Methods

Sample Preparation

Expression of proteins was carried out using *E. coli* BL21(DE3) cells grown in ~100% D_2O-based M9 minimal media, containing ^{15}N-ammonium chloride (1 g/L) and [^{2}H,^{12}C]-glucose (3 g/L) as the sole nitrogen and carbon sources, respectively. Specifically labeled precursors[1,2] were added 1 h prior to the induction of protein overexpression with 1 mM IPTG, as described previously.[2,3] Purification of samples followed literature protocols. The following samples were used: (i) 1.5 mM [U-^{2}H; Ileδ1-$^{13}CH_3$; Leu,Val-$^{13}CH_3$/$^{12}CD_3$; Met-$^{13}CH_3$]-labeled B1 domain of immunoglobulin binding protein G (referred to as GB1)[4] in 50 mM potassium phosphate pH 7.5, 100 mM NaCl, 0.1 mM NaN_3, 100% D_2O; (ii) 1.5 mM [U-^{2}H; Ileδ1-$^{13}CH_3$; Leu,Val-$^{13}CH_3$/$^{12}CD_3$; Met-$^{13}CH_3$]-labeled FF domain from human HYPA/FBP11[5] in 25 mM potassium phosphate pH 6.8, 50 mM NaCl, 1 mM EDTA, 100% D_2O; (iii) 0.9 mM (monomer concentration) [U-^{2}H; Ileδ1-$^{13}CH_3$; Leu,Val-$^{13}CH_3$/$^{12}CD_3$; Met-$^{13}CH_3$]-labeled $\alpha_7\alpha_7$, from *T. acidophilum*,[6] 25 mM potassium phosphate pH 7.4, 50 mM NaCl, 4.6 mM NaN_3, 1 mM EDTA, 100% D_2O; (iv) 0.5 mM (monomer concentration) [U-^{2}H; Ileδ1-$^{13}CH_3$; *proR*, Leu,Val-$^{13}CH_3$/$^{12}CD_3$; Met-$^{13}CH_3$]-labeled ND1Lp97-ADP R95G (referred to as R95G-p97), from *Mus musculus* (identical to that from *Homo sapiens*),[2,7] 25 mM HEPES pH 7.4, 50 mM NaCl, 5 mM ADP, 4 mM TCEP, 100% D_2O. The level of deuteration in all samples was > 95% at all carbon sites. A high level of deuteration is important to avoid ^{1}H–^{1}H scalar-coupled evolution during the CPMG pulse train.

NMR Spectroscopy

All NMR experiments were recorded on Bruker AVANCE III 600 MHz and 800 MHz spectrometers equipped with cryogenically cooled probes with triple-axis pulsed field gradients. ^{1}H SQ-CPMG data sets were measured at 5 °C for GB1, 25 °C for the FF domain, 50 °C for $\alpha_7\alpha_7$ and R95G-p97. ^{13}C MQ-CPMG, ^{13}C SQ-CPMG, ^{1}H SQ-CPMG (I = 1/2) and ^{1}H TQ-CPMG datasets were recorded as described previously in the lit-

erature.[8–11] Note that the ^{1}H SQ-CPMG (I = 1/2) scheme selects only magnetization components from the I = 1/2 manifold, eliminating artifacts associated with interchange between fast and slow relaxing magnetization components, at the expense of approximately an order of magnitude in sensitivity.[10] ^{1}H relaxation dispersion experiments have been recorded using a constant-time CPMG element[12,13] with T_{relax} = 30 ms (GB1 and FF domain) or 15 ms ($\alpha_7\alpha_7$ and R95G-p97). Experiments were recorded as pseudo-3D datasets by varying the number, N, of CPMG pulses during T_{relax} (1 N value for each 2D plane), with the parameter N_{max} set as the maximum value of N. A series of 2D maps was obtained with ν_{CPMG} values varying between 33 Hz (T_{relax} = 30 ms) or 67 Hz (T_{relax} = 15 ms) and 2000 Hz. Approximately 20–30 planes were recorded for each dispersion series, including duplicates for error analysis.[14] The total measurement time for each experiment at each magnetic field was ~3 h (GB1), ~5 h (FF domain) or ~70 h ($\alpha_7\alpha_7$ and R95G-p97).

Discussion

Details of ^{1}H SQ-CPMG Pulse Sequence

(i) Practical aspects

All 90° (180°) rectangular pulses are denoted by narrow (wide) bars. These are applied at maximum power, with exception of the ^{1}H pulses during the CPMG element (pulses of phase ψ_1, ψ_2 and ϕ_2) that use a ~25 kHz field. All pulses are applied along the x-axis unless otherwise indicated. The ^{1}H CPMG pulses are applied as either single 180° or $90^\circ_x240^\circ_y90^\circ_x$[15] composite pulses; the latter is, in general, preferred due to improved off-resonance performance (Figure S1). The water-selective shaped pulse marked with "w" (~7 ms) is implemented using the EBURP-1 profile.[16] A single $180^\circ_{\phi_2}$ pulse is applied in the center of the CPMG scheme that decreases the effects of pulse imperfections, as described previously.[17] ^{1}H and ^{13}C carriers are placed in the center of the methyl region (~1 ppm and ~20 ppm, respectively), with the ^{1}H carrier positioned at the water resonance (~4.7 ppm) during application of the water selective

pulse. ^{13}C WALTZ-16 decoupling[18] is applied with a field of ~2 kHz during acquisition (t_2). The delays used are: τ_a = 2.0 ms, $\tau_{cp} = (T_{\mathrm{relax}} - 2 \times pwh\_180 \times N_{\mathrm{max}})/(4N)$ where *pwh*_180 is the length of each refocusing CPMG pulse (see pulse code). The phase cycle used is $\phi_1 = \mathrm{x}, -\mathrm{x}$; $\phi_2 = 2(\mathrm{y}, \mathrm{y}, -\mathrm{y}, -\mathrm{y}), 2(-\mathrm{y}, -\mathrm{y}, \mathrm{y}, \mathrm{y})$; $\phi_{\mathrm{rec}} = \mathrm{x}, -\mathrm{x}$. A minimum phase cycle of 4 steps is required. The cyan or orange pulse is applied in successive scans (only one per scan; see pulse sequence code). The phases ψ_1/ψ_2 are used to implement the XY-4 scheme[19] that is applied to the CPMG pulses. This phase cycle, along with the central pulse of phase ϕ_2 in Figure 2A which is also cycled, compensate for pulse imperfections caused by both off-resonance effects and miscalibration. Notably, in tests of the robustness of the CPMG scheme to errors in pulse settings we have found that when CPMG pulses are deliberately misset by 3% there are no changes to dispersion profiles; in our experience ^{1}H pulses can be calibrated to a precision significantly higher than this, on the order of 0.1 μs for 360° pulses. Phase ψ_1 is incremented with the cycle $(\mathrm{x}, \mathrm{y}, \mathrm{x}, \mathrm{y})$ for each successive pulse, with ψ_2 decremented in the same manner, but inverted. Thus, the CPMG element becomes

$$\tau_{cp}\Pi_1\tau_{cp}\tau_{cp}\Pi_2\tau_{cp}\ldots\tau_{cp}\Pi_{N-1}\tau_{cp}\tau_{cp}\Pi_N\tau_{cp}\Pi_{N+1}\ldots\Pi_{N_{\mathrm{max}}}180^\circ_{\phi_2}\overline{\Pi}_{N_{\mathrm{max}}}\ldots\overline{\Pi}_{N+1}\tau_{cp}\overline{\Pi}_N\tau_{cp}\tau_{cp}\overline{\Pi}_{N-1}\tau_{cp}\ldots\tau_{cp}\overline{\Pi}_2\tau_{cp}\tau_{cp}\overline{\Pi}_1\tau_{cp}$$

where $\Pi_1 = \Pi_{\mathrm{x}}$, $\Pi_2 = \Pi_{\mathrm{y}}$, $\Pi_3 = \Pi_{\mathrm{x}}$ and so on following the XY-4 scheme, with $\Pi_{\mathrm{x}} = 90^\circ_{-\mathrm{y}}240^\circ_{\mathrm{x}}90^\circ_{-\mathrm{y}}$, $\Pi_{\mathrm{y}} = 90^\circ_{\mathrm{x}}240^\circ_{\mathrm{y}}90^\circ_{\mathrm{x}}$. $\overline{\Pi}_{\mathrm{j}}$ values are calculated from Π_{j} by interchanging $\mathrm{y}(-\mathrm{y})$ with $-\mathrm{y}(\mathrm{y})$ in expressions for Π_{j}, that follows from the $180^\circ_{\phi_2}$ pulse in the center of the pulse scheme, as discussed by Hansen et al.[17] Quadrature detection in F_1 is achieved by STATES–TPPI of ϕ_1.[20] Gradients are applied with the following durations (ms) and strengths (in % maximum): g_1: (1.0, 20%), g_2: (0.5, 30%). An additional 3-9-19 WATERGATE element[21] prior to t_2 acquisition can be applied to achieve higher degree of water suppression that is necessary for applications involving proteins dissolved in $^1\mathrm{H}_2\mathrm{O}$.

(ii) Suppressing the effects of differential relaxation between in-phase and anti-phase ^{1}H SQ magnetization

During a CPMG pulse train ^{1}H magnetization evolves between in-phase and anti-phase components that can have, in some cases, significantly different effective relaxation

rates. This is particularly the case in the context of ^{15}N- or ^{13}C-CPMG pulse trains where, in applications to biomolecules, there is a significant contribution to the relaxation of heteronuclear magnetization that is anti-phase with respect to coupled ^{1}H spins from ^{1}H–^{1}H cross-relaxation.[22] In the present application differential relaxation rates for ^{1}H magnetization in-phase or anti-phase with respect to the one-bond coupled ^{13}C spin are expected, although these should be small (see below). Loria, Rance and Palmer have developed an elegant approach whereby in-phase/anti-phase magnetization components are exchanged in the center of the CPMG scheme, so that the effective relaxation of magnetization becomes independent of J-evolution[23] (*i.e.*, independent of the number of CPMG pulses). That is, for example, magnetization starting as in-phase for the first half of the CPMG train is subsequently converted to anti-phase to start the second half. In general, an even number of CPMG pulses must be applied in each half of the CPMG train. Here we have used a slightly different scheme, Figure 2A, that enables either odd or even numbers of CPMG pulses to be used in each CPMG half, and that works well so long as differential relaxation between in-phase and anti-phase components is small, as is the case for ^{1}H magnetization (see below). This is accomplished by inserting a delay $\tau_a = 1/(4J_{HC})$, where J_{HC} is the one-bond ^{1}H–^{13}C scalar coupling constant, immediately after the ^{13}C pulse at the end of the t_1 interval, creating equal amounts of in-phase and anti-phase ^{1}H components. In order to have a scheme that works for both odd and even numbers of CPMG pulses (*i.e.*, any integer number of N in the scheme of Figure 2A) an additional modification must be made. Consider first the CPMG element of Figure 2A without the cyan pulse. After the τ_a period that follows ^{13}C t_1 evolution the signal of interest is given by $\sin(\pi J_{HC}\tau_a)I_y + \cos(\pi J_{HC}\tau_a)2I_xC_z$, assuming that the I spin of interest is on-resonance and ignoring both relaxation and the effects of the g_2 gradient pair, where I and C are proton and carbon spin operators, respectively. Evolution during the first τ_{cp} element then generates

$$I_y s + 2I_xC_z c \xrightarrow{\tau_{cp}} I_y \sin(\frac{\pi}{4} + \pi J_{HC}\tau_{cp}) + 2I_xC_z \cos(\frac{\pi}{4} + \pi J_{HC}\tau_{cp}) \qquad \text{(S1)}$$

where $s = \sin(\pi J_{HC}\tau_a)$ and $c = \cos(\pi J_{HC}\tau_a)$. Note that during this τ_{cp} period there

is 'more' in-phase than anti-phase magnetization so that the effective relaxation rate is skewed towards the in-phase decay. Assuming rapid interconversion between in-phase and anti-phase components ($2\pi J_{HC} \gg |\Delta|$) the effective relaxation during the τ_{cp} interval is single exponential with a calculated rate of $R_2 + (\frac{1}{2} + x)\Delta$, where R_2 is the ^{1}H in-phase decay, $\Delta = R_{2I_xC_z} - R_2$ is the difference in relaxation rates between anti-phase and in-phase ^{1}H magnetization and $x = \frac{1}{4\pi J_{HC}\tau_{cp}}(\cos(2\pi J_{HC}\tau_{cp}) - 1)$. Application of the first refocusing pulse, followed by evolution during the second τ_{cp} period refocuses J-evolution and magnetization decays with the same average rate as in the first interval. For the case where N is even the magnetization at the start of the second $\tau_{cp} - 90^\circ_{\theta-\pi/2}240^\circ_\theta 90^\circ_{\theta-\pi/2} - \tau_{cp}$ element (*i.e.*, at the start of the 3rd τ_{cp}) is proportional to $I_y s - 2I_x C_z c$ that evolves under scalar coupling during the subsequent τ_{cp} delay as

$$\begin{aligned} I_y s - 2I_x C_z c \xrightarrow{\tau_{cp}} & I_y \sin(\frac{3\pi}{4} + \pi J_{HC}\tau_{cp}) + 2I_x C_z \cos(\frac{3\pi}{4} + \pi J_{HC}\tau_{cp}) \\ & = I_y \cos(\frac{\pi}{4} + \pi J_{HC}\tau_{cp}) - 2I_x C_z \sin(\frac{\pi}{4} + \pi J_{HC}\tau_{cp}) \end{aligned} \quad \text{(S2)}$$

Now the effective relaxation rate becomes skewed towards the decay of anti-phase magnetization as τ_{cp} grows because the amount of anti-phase magnetization exceeds the in-phase component. Under the assumption of rapid interconversion between in-phase and anti-phase magnetization elements, the effective relaxation rate is calculated to be $R_2 + (\frac{1}{2} - x)\Delta$ for this second spin echo period. The net relaxation rate, averaged over the two echoes, is thus $0.5\{R_2 + (\frac{1}{2} + x)\Delta + R_2 + (\frac{1}{2} - x)\Delta\} = R_2 + \frac{1}{2}\Delta$, independent of x, and this holds for all even values of N. In contrast, when N is odd the effective relaxation rate does not average to be independent of x; in the case of N = 1, for example, the effective relaxation rate for the total CPMG train is given by $R_2 + (\frac{1}{2} + x)\Delta$ that differs from the rate obtained when N is even.

The solution is to record a second scan with the cyan, but not the orange pulse, inserted (the first scan would include the orange pulse so that an odd number of pulses is maintained between the g_2 gradient pair). In this case the initial magnetization (start of the first τ_{cp} period) is proportional to $I_y s - 2I_x C_z c$ and the effective relaxation rate for the first echo is given by $R_2 + (\frac{1}{2} - x)\Delta$. An argument similar to that above establishes that

for even values of N the effective relaxation rate over a pair of spin echoes is independent of x. However, for odd N the effective rate is now skewed towards the rate for the anti-phase component. Consider the case of $N = 1$, then the effective relaxation rate for the total CPMG train is given by $R_2 + (\frac{1}{2} - x)\Delta$. Addition of a pair of scans, corresponding to with and without the cyan pulse, thus gives a signal,

$$e^{-(R_2+(\frac{1}{2}-x)\Delta)T_{\text{relax}}} + e^{-(R_2+(\frac{1}{2}+x)\Delta)T_{\text{relax}}} = e^{-(R_2+\frac{\Delta}{2})T_{\text{relax}}}\{e^{x\Delta T_{\text{relax}}} + e^{-x\Delta T_{\text{relax}}}\} \qquad \text{(S3)}$$

for odd N values and so long as $|x\Delta T_{\text{relax}}| \ll 1$ the effective relaxation rate is $R_2 + \frac{1}{2}\Delta$. We have measured Δ values of 0.89 ± 0.58 s^{-1} for GB1 (5 °C, 16 methyl groups ranging from 0.17 s^{-1} to 2.72 s^{-1}), and -1.24 ± 1.26 s^{-1} for $\alpha_7\alpha_7$ (50 °C, 77 methyl groups from -5.73 s^{-1} to 1.38 s^{-1}) at 600 MHz; 0.75 ± 0.53 s^{-1} (0.16 s^{-1} to 2.30 s^{-1}) and -0.35 ± 1.41 s^{-1} (-4.32 s^{-1} to 3.82 s^{-1}) for GB1 and $\alpha_7\alpha_7$, respectively, at 800 MHz. For these values of Δ and for typical T_{relax} values, $|x\Delta T_{\text{relax}}| \ll 1$.

The above discussion is germane for small CPMG pulse rates where the rate of interconversion between in-phase and anti-phase magnetization components is large relative to the difference in their relaxation rates ($|\Delta|$). As ν_{CPMG} increases there is less interconversion between in-phase and anti-phase magnetization, with each component thus relaxing independently. As equal amounts of each component are present initially the relaxation becomes bi-exponential, with the magnetization given by,

$$\frac{1}{2}e^{-R_2T_{\text{relax}}} + \frac{1}{2}e^{-(R_2+\Delta)T_{\text{relax}}} = \frac{1}{2}e^{\frac{\Delta T_{\text{relax}}}{2}}e^{-(R_2+\frac{\Delta}{2})T_{\text{relax}}} + \frac{1}{2}e^{-\frac{\Delta T_{\text{relax}}}{2}}e^{-(R_2+\frac{\Delta}{2})T_{\text{relax}}} \qquad \text{(S4)}$$

and so long as $\left|\frac{\Delta T_{\text{relax}}}{2}\right| \ll 1$ the relaxation is single exponential with a rate of $R_2 + \frac{\Delta}{2}$, independent of x. Simulations that we have performed show that flat profiles are obtained for $|\Delta| \leq 5$ s^{-1}. Note that the scheme of Loria, Rance and Palmer[23] is, in general, more effective than the one used here because in-phase and anti-phase components are interchanged by an element in the middle of the CPMG train, ensuring that magnetization decay is single exponential. But the approach used here may be preferred for ^{1}H CPMG schemes because $|\Delta|$ is small (smaller than for ^{15}N or ^{13}C CPMG, espe-

cially in the case of protonated proteins) and the present implementation ensures that both odd and even numbers of CPMG pulses can be used.

It is worth noting that the scheme of Figure 2A places the ^{13}C evolution period prior to the ^{1}H CPMG element. As described by Ishima and Torchia,[24] so long as the ^{13}C chemical shifts of proximal methyl protons are not degenerate the protons behave as unlike spins (more favorable relaxation properties) irrespective of ν_{CPMG}, minimizing spurious dispersion profiles that might otherwise arise as cross-relaxing spins shift from unlike to like with high CPMG pulsing rates. We have not observed any cross-peaks in CPMG spectra that would be diagnostic of magnetization exchange due to ^{1}H–^{1}H cross-relaxation, even for the large systems considered here ($\alpha_7\alpha_7$ and R95G-p97).

Data Analysis

All NMR spectra have been processed and analyzed using the *NMRPipe*.[25] Effective transverse relaxation rates, $R_{2,\mathrm{eff}}$, were calculated based on peak intensities according to the relation $R_{2,\mathrm{eff}}(\nu_{\mathrm{CPMG}}) = -\ln(I(\nu_{\mathrm{CPMG}})/I_0)/T_{\mathrm{relax}}$, where I_0 is the peak intensity in a reference spectrum recorded without the relaxation delay, T_{relax}.[12] Fitting of cross-peaks in CPMG data sets was carried out using the software package *ChemEx* (https://github.com/gbouvignies/chemex) that included a separate module required for the ^{1}H SQ-CPMG relaxation dispersion data. The module is available from the authors upon request. Residues were only included in the analysis if their dispersion profiles satisfied $R_{\mathrm{ex}} = R_{2,\mathrm{eff}}(\nu_{\mathrm{CPMG}} = x\ \mathrm{Hz}) - R_{2,\mathrm{eff}}(\nu_{\mathrm{CPMG}} = 2000\ \mathrm{Hz}) > 1\ \mathrm{s}^{-1}$ at 800 MHz, with x = 33 Hz and 67 Hz for experiments recorded with T_{relax} = 30 ms (GB1 and FF domain) or 15 ms ($\alpha_7\alpha_7$ and R95G-p97), respectively. Exchange parameters were extracted from fits of dispersion data to a two-site exchange model using the Bloch–McConnell equations,[26] as described previously.[14] The fitting parameters include the global values p_E and k_{ex} (or alternatively $k_{EG} = (1 - p_E)k_{\mathrm{ex}}$ and $k_{GE} = p_E k_{\mathrm{ex}}$), residue-specific chemical shift differences, $\Delta\varpi_{GE}$ (ppm), and the intrinsic SQ ^{1}H relaxation rates for the exchanging spins.

The ^{13}C SQ-CPMG, ^{1}H SQ-CPMG and ^{1}H TQ-CPMG datasets for the FF do-

main were measured at both 600 MHz and 800 MHz, while for R95G-p97 only a single ^{1}H SQ-CPMG dataset was measured at 800 MHz. In this case p_E was fixed to the value determined previously based on ^{13}C MQ-CPMG data (10%),[7] to yield $k_{ex} = 2500 \pm 200$ s^{-1}.

Numerical Simulations

As described in the text, magnetization components evolve during the CPMG refocusing pulses, interconverting between fast and slow relaxing elements. This has the effect of (i) decreasing the inherent sensitivity of the experiment and of (ii) generating artifacts unless the number of pulses during the CPMG train is fixed. Artifacts are further suppressed using composite pulses of the $90^\circ_{\theta-\pi/2}240^\circ_\theta 90^\circ_{\theta-\pi/2}$ variety with XY-4 phase cycling (see Figure 2A). Figures 1C,D illustrate the interconversion of density elements for the simple case where relaxation is neglected and pulses are on-resonance, applied with a 20 kHz field. We consider the energy level diagram of an X_3 spin system (Figure 1B), with separation of levels according to the net spin angular momentum (I) of each state $|j\rangle$ and highlight ^{1}H SQ, DQ and TQ coherences. Note that SQ (blue, red), DQ (green) and TQ (magenta) coherences can be excited within the spin 3/2 manifold and that the single quantum transitions denoted by red and blue relax very differently in the macromolecular limit.[27,28] These have been labeled as SQ_{fast} (red, fast relaxing) and SQ_{slow} (blue, slow relaxing). Diagonal elements are not depicted but correspond to density terms $|j\rangle\langle j|$. For the purposes of illustration we consider only the I = 3/2 manifold and start with SQ_{slow}. The plots in Figures 1C,D were generated by propagating the Liouville–von Neumann equation for the spin-3/2 manifold using the basis functions for the 4×4 density matrix, $\rho_{ij} = |i\rangle\langle j|$. In the starting density matrix, $\rho(0)$, the elements corresponding to the SQ_{slow} transitions are each set to $1/\sqrt{2}$, $\rho_{23}(0) = \rho_{32}(0) = 1/\sqrt{2}$ and all other elements are set to 0. The density elements are defined as follows: $M^2_{Diag} = \rho^2_{11} + \rho^2_{22} + \rho^2_{33} + \rho^2_{44}$, $M^2_{SQ_{fast}} = \rho^2_{12} + \rho^2_{21} + \rho^2_{34} + \rho^2_{43}$, $M^2_{SQ_{slow}} = \rho^2_{23} + \rho^2_{32}$, $M^2_{DQ} = \rho^2_{13} + \rho^2_{31} + \rho^2_{24} + \rho^2_{42}$, $M^2_{TQ} = \rho^2_{14} + \rho^2_{41}$ and $\rho^2_{ij} = \rho^*_{ij}\rho_{ij}$.[29] Note that the sum $M^2_{Diag} + M^2_{SQ_{fast}} + M^2_{SQ_{slow}} + M^2_{DQ} + M^2_{TQ}$ is constant during the pulse.

Two simulations were performed for each pulse, corresponding to refocusing pulse phases of x and y, and the results averaged to generate the profiles shown in the figure.

A second set of simulations was performed to illustrate the evolution of magnetization during the course of the CPMG pulse train, starting with SQ_{slow} of the 3/2 manifold, neglecting relaxation and assuming a non-exchanging system. In these simulations the CPMG scheme of Figure 2A was used where each refocusing pulse was either a single 180° pulse (Figures S1A–C) or a composite $90^\circ_{\theta-\pi/2}240^\circ_{\theta}90^\circ_{\theta-\pi/2}$ pulse (Figures S1D–F) applied with the XY-4 phase cycle or constant phase. Because relaxation was not included in the simulations the cyan or orange pulse in Figure 2A was omitted, as were the pulse trains ($N_{\max} - N$ pulses) that would normally compensate for relaxation during the CPMG pulses. Evolution of the density elements was carried out as described above, with the inclusion of additional chemical shift propagation during the τ_{cp} periods separating the pulses, assuming an offset of 1 kHz for the ^{1}H spin of interest from the carrier and a 20 kHz ^{1}H field. Three cases were considered, corresponding to N = 4, 20 and 40, where N is the number of pulses in each CPMG train on either side of the central $180^\circ_{\phi_2}$ pulse (see Figure 2A). Thus, for N = 4 a total of 8 pulses were applied over a constant time interval, T_{relax}, of 40 ms and $M^2_{SQ_{slow}}$ calculated at each echo (dots in Figure S1).

As described above relaxation losses ensue during the application of CPMG refocusing pulses since magnetization is interconverted between fast and slow relaxing elements. In order to quantify how much the losses might be we simulated CPMG profiles using both single and composite pulses with relaxation explicitly included. Relaxation rates of the density elements were calculated using literature expressions and included in the Liouvillian that describes the time evolution of the density matrix.[29] During the periods between refocusing pulses (τ_{cp}) the evolution of density matrix was evaluated as $\rho(t+\tau_{cp}) = \rho(t)\exp(-iL\tau_{cp})$, where L is the Liouvillian representing free precession. The same expression was also used to evaluate density matrix evolution during the CPMG pulses, with the Liouvillian including additional contributions from RF pulses.

Chemical exchange was not considered so that flat lines are expected. Figure S6 shows the results of the simulations. As expected $R_{2,\mathrm{eff}}$ values are larger in the case of the composite pulses relative to the simple pulses, due to their longer duration (and hence more interconversion between differentially relaxing elements during the pulses). Finally, we were also interested in establishing how the compensating pulse trains of Figure 2A ($N_{\mathrm{max}} - N$ pulses) influence the sizes of dispersion profiles when differential relaxation between different density elements is neglected. This is more of an academic question, because as we have shown these trains are necessary to ensure that dispersions are robust to artifacts that would otherwise emerge from relaxation during the CPMG pulses. Figure S7 shows simulations of CPMG trains that do not include spin relaxation so that the effects of the compensation pulses on how the exchange process is 'read out' can be elucidated. Note that the exact CPMG element is used in our fitting software so that the complete experimental pulse train is taken into account.

Supplementary Figures

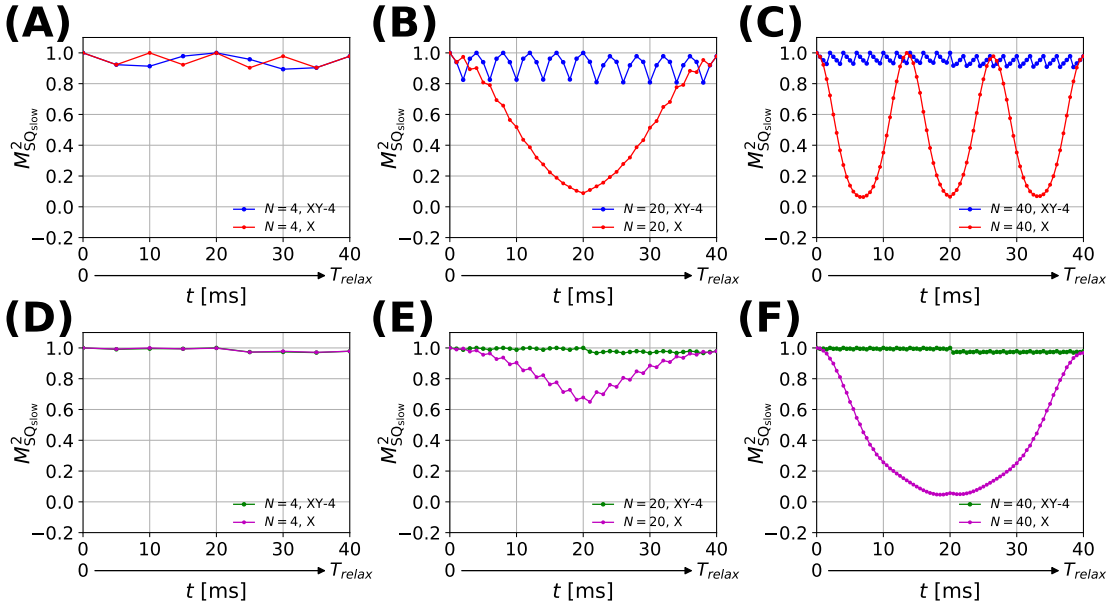

Figure S1. Numerical simulations showing the evolution of $M^2_{\mathrm{SQ_{slow}}}$ during the CPMG pulse train (duration T_{relax}) of Figure 2A. Each circle in the profiles corresponds to the value of $M^2_{\mathrm{SQ_{slow}}}$ after successive single spin-echoes, $\tau_{cp} - 180^\circ - \tau_{cp}$. For example, in panel A, $N = 4$, $T_{\mathrm{relax}} = 40$ ms so that the duration of each $\tau_{cp} - 180^\circ - \tau_{cp}$ element is 5 ms (see Figure 2A). Note that the ideal situation occurs when the trajectory of magnetization is flat (*i.e.*, $M^2_{\mathrm{SQ_{slow}}} \sim 1$ throughout the complete trajectory). Details of the simulation are described above, focusing only on the $I = 3/2$ manifold, and it is assumed that only the x-component of $\mathrm{SQ_{slow}}$ magnetization is initially present. All simulations are performed with a ^{1}H B_1 field of 20 kHz and a ^{1}H offset of 1 kHz. Relaxation and chemical exchange are not included so that flat dispersion profiles are expected in the absence of pulse imperfections (offset effects). In each simulation CPMG pulses are applied with the XY-4 phase cycle (blue in A–C; green in D–F) or with constant phase along x (red in A–C, magenta in D–F) with single 180° (A–C) or $90^\circ_x 240^\circ_y 90^\circ_x$ composite CPMG pulses (D–F). Note that when the XY-4 scheme is used $M^2_{\mathrm{SQ_{slow}}}$ is refocused after every 4 pulses. This is especially obvious in A–C (blue), while in D–F there are only small fluctuations from 1.0 when the XY-4 cycle is used (green). Much larger deviations are observed when single 180° pulses are employed.

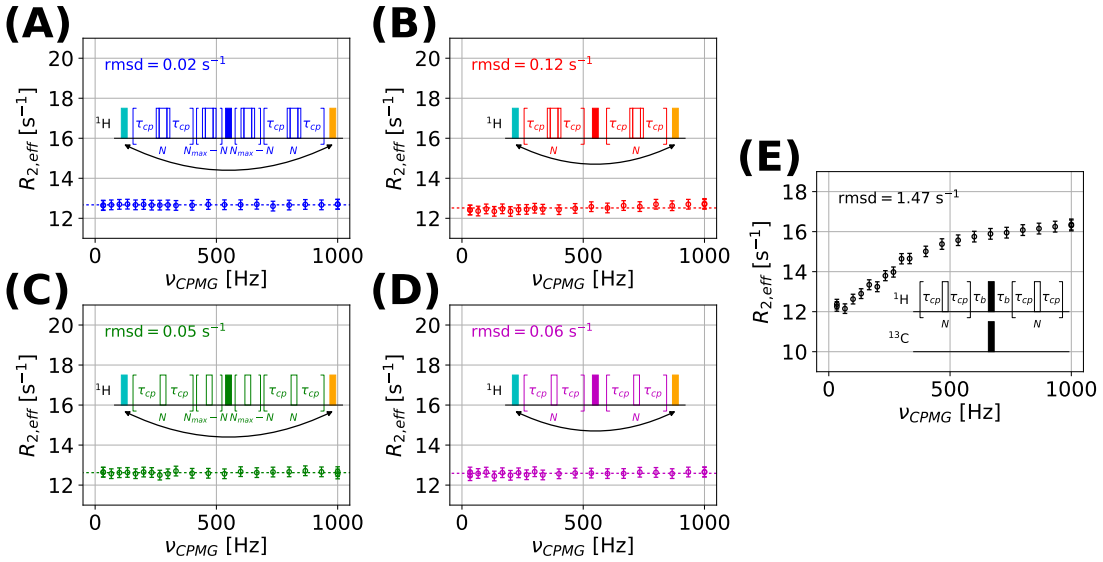

Figure S2. ^{1}H SQ-CPMG dispersion profiles measured on residue V21γ2 of GB1 at 5 °C using several different CPMG schemes, as illustrated in each panel. (A) $90^\circ_x240^\circ_y90^\circ_x$ composite CPMG pulses with relaxation compensation trains comprising $N_{\max} - N$ pulses: this is the scheme of Figure 2A; (B) $90^\circ_x240^\circ_y90^\circ_x$ composite CPMG pulses without relaxation compensation elements; (C) single 180° CPMG pulses with relaxation compensation elements; (D) single 180° CPMG pulses without relaxation compensation elements; (E) single 180° CPMG pulses with constant phase along x or y in each pulse train, and with a central element to suppress the effects of differential relaxation between in-phase and anti-phase ^{1}H SQ coherences.[30] The value of τ_b is set to $1/(4J_{HC})$. In A–D the XY-4 cycle has been used. RMSD values from fits of the dispersion curves (circles) to flat lines are indicated; these tend to be slightly larger for profiles measured without compensation elements since $R_{2,\text{eff}}$ increases slightly with ν_{CPMG}. However, for GB1 with a relatively small molecular weight ($\tau_C \sim 10$ ns at 5 °C) such effects are negligible. This is not the case for larger proteins, such as those highlighted in the main text where the scheme of Figure 2A is required to completely suppress artifacts.

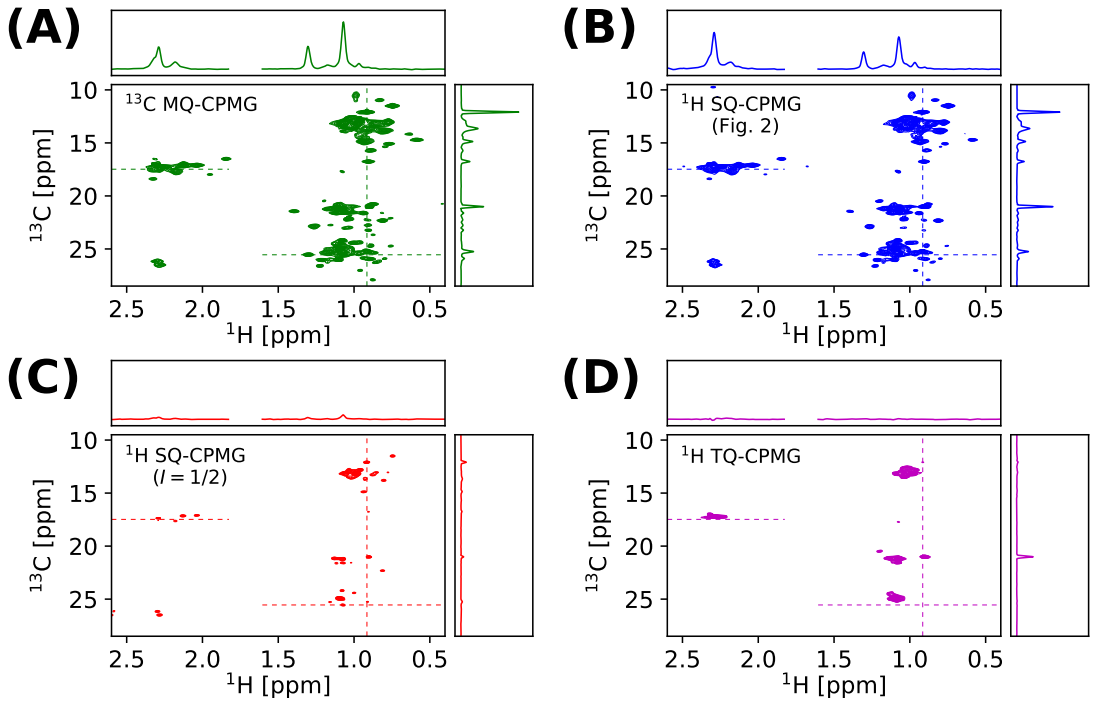

Figure S3. ^{1}H–^{13}C HMQC correlation maps for R95G-p97 recorded at 800 MHz and 50 °C using the following schemes: (A) ^{13}C MQ-CPMG;[8] (B) ^{1}H SQ-CPMG, Figure 2A; (C) ^{1}H SQ-CPMG (I = 1/2);[10] (D) ^{1}H TQ-CPMG.[11] All spectra were measured with T_{relax} = 15 ms, ν_{CPMG} = 2 kHz with identical delay times and scans, and are plotted at the same contour level (~10 times of the average spectral noise). Horizontal or vertical dashed lines indicate the position where 1D cross-sections are taken at specific ^{13}C or ^{1}H offsets. In general the sensitivity of correlations in spectra recorded with the ^{13}C MQ-CPMG scheme is higher than for the ^{1}H SQ-CPMG of Figure 2A, reflecting losses during the compensation pulses in the ^{1}H experiment (see Figure S6).

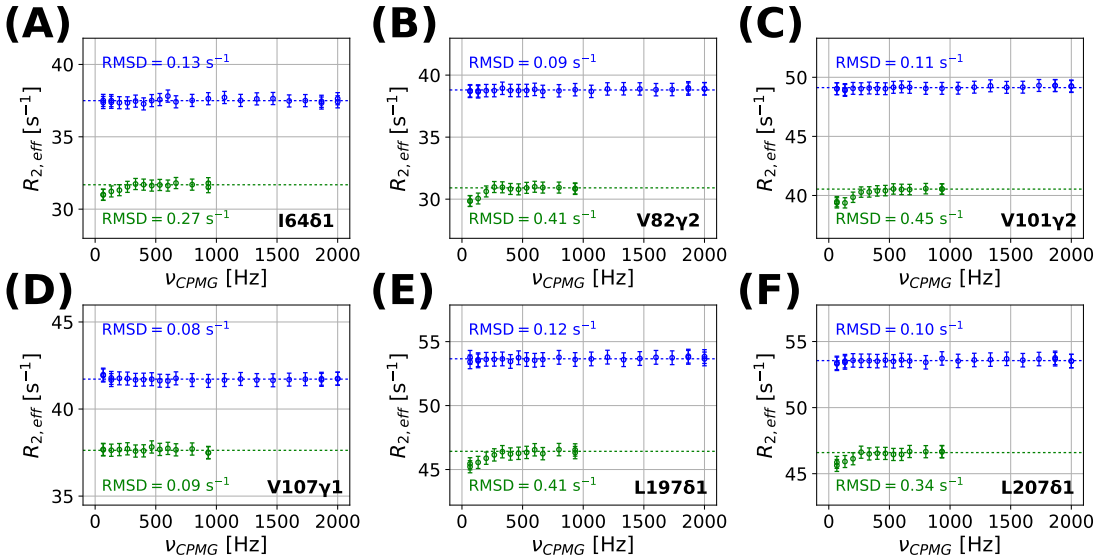

Figure S4. Additional examples of ^{1}H SQ-CPMG dispersion profiles measured for $\alpha_7\alpha_7$ at 800 MHz and 50 °C (as in Figure 1A). Profiles are obtained with either $90^{\circ}_{x}240^{\circ}_{y}90^{\circ}_{x}$ composite pulses (blue) or single 180° pulses (green) using the CPMG elements highlighted in panels A and C of Figure S2, respectively. Notably, dispersion profiles measured with single 180° pulses increase slightly for $\nu_{\mathrm{CPMG}} \leq 300$ Hz. For systems in relatively fast exchange where $\nu_{\mathrm{CPMG}} > 300$ Hz are used throughout (exchange rates > 1500–2000 s^{-1}), single pulses are recommended as artifacts are minimal and relaxation during the pulses is reduced because of their shorter duration in relation to their composite counterparts. In both experimental datasets a compensation scheme (see Figure 2A) was used ensuring that the same number of refocusing pulses are applied, independent of ν_{CPMG}. In the absence of such a compensation approach dispersion profiles increase significantly with pulsing frequency, as illustrated in Figure 1A (black, red).

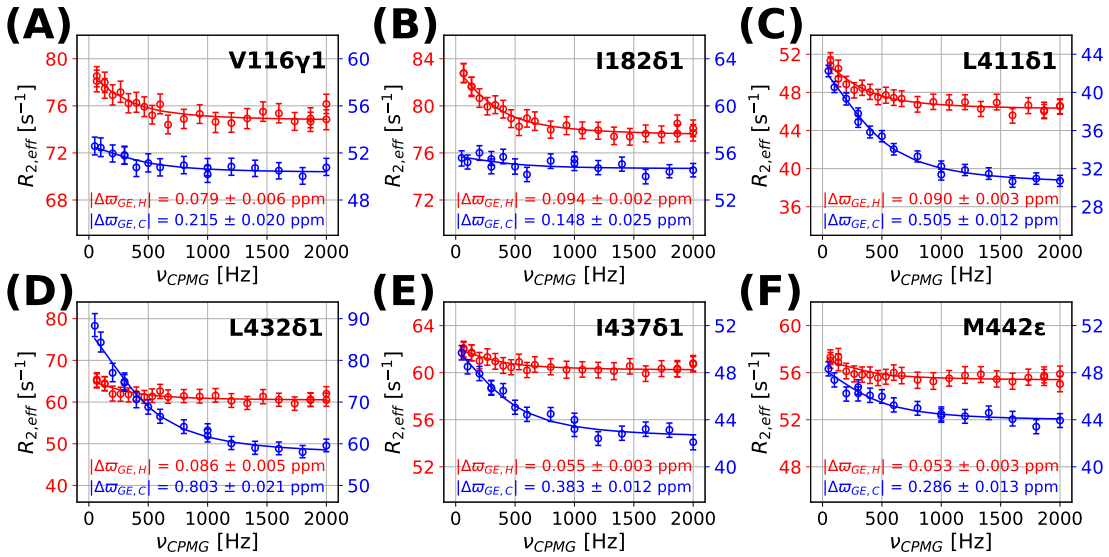

Figure S5. Further examples of ^{1}H SQ-CPMG (red) and ^{13}C MQ-CPMG (blue) dispersion profiles measured on R95G-p97 at 800 MHz, 50 °C. These ^{1}H dispersions, along with those in Figure 3 were included in a global fit to quantify k_{ex} (2500 ± 200 s^{-1}). The extracted k_{ex} value from the ^{1}H data is in excellent agreement with the fitted k_{ex} from ^{13}C dispersions (~2700 s^{-1}); values of $|\Delta\varpi_{GE,C}|$ were obtained from fits of the ^{13}C dispersion profiles and are listed in the panels, along with $|\Delta\varpi_{GE,H}|$ values that were obtained from analysis of ^{1}H dispersions. The assignments listed are tentative as (near) complete assignments are available only for the WT, ADP-p97 state but not for the R95G mutant.

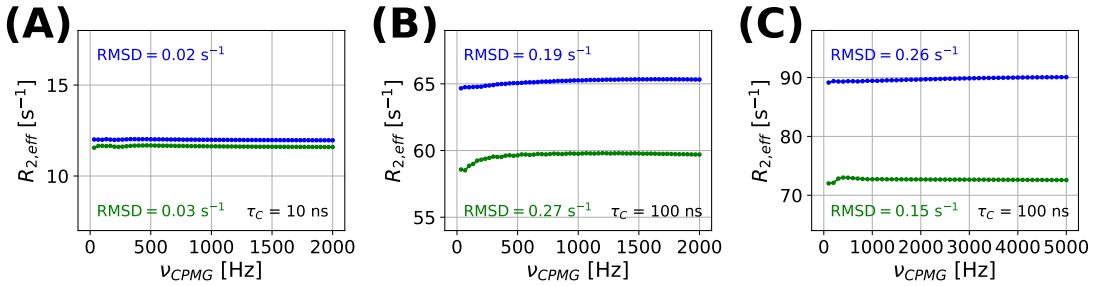

Figure S6. Simulated ^{1}H SQ-CPMG dispersion profiles with either $90^{\circ}_{x}240^{\circ}_{y}90^{\circ}_{x}$ composite (blue) or single 180° (green) pulses and including relaxation. In the simulations methyl ^{1}H–^{13}C and ^{1}H–^{1}H bond lengths of $r_{HC} = 1.135$ Å and $r_{HH} = 1.813$ Å[31] were used, along with effective distances of $r_{HH,\text{ext}} = 3.5$ Å and $r_{HD,\text{ext}} = 1.8$ Å to single external ^{1}H and ^{2}H spins that are intended to take into account all ^{1}H–^{1}H and ^{1}H–^{2}H external dipolar relaxation effects.[31] The order parameters squared, S^2, for intra-methyl and external sources of dipolar relaxation are 0.5 and 1.0, respectively. All simulations were carried out with a ^{1}H B_1 field of 20 kHz and a ^{1}H offset of 1 kHz. Molecular tumbling times were τ_C = 10 ns (panel A) or τ_C = 100 ns (panel B, C). In panel (A, B) T_{relax} = 30 ms and N_{max} = 60, while in panel (C) T_{relax} = 10 ms and N_{max} = 50. Chemical exchange is not included in the simulation. Individual simulations are performed for the I = 3/2 and I = 1/2 manifolds separately, with signals from both manifolds subsequently added to obtain the final results.

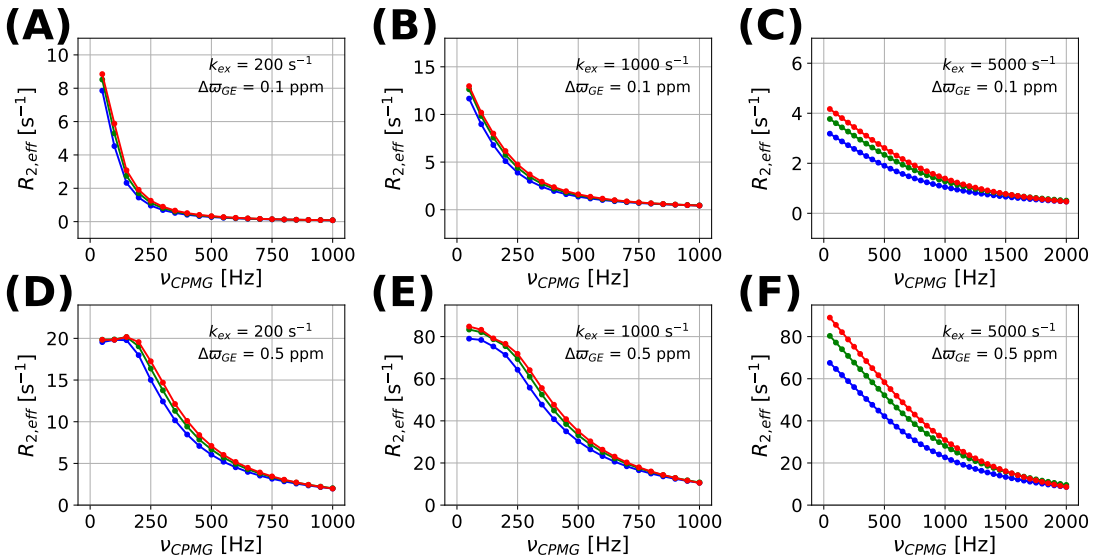

Figure S7. Simulated ^{1}H SQ-CPMG dispersion profiles evaluating how the compensation trains of duration $N_{\max} - N$ pulses (Figure 2A) affect relaxation dispersion profile sizes. The following parameters are used for the simulation, T_{relax} = 20 ms and p_E = 0.10, k_{ex} = 200, 1000 and 5000 s^{-1} (shown in each panel), $\Delta\varpi_{GE}$ = 0.1 ppm and 0.5 ppm (shown in each panel), all pulses are on-resonance with the ground state and applied with a 20 kHz field. Relaxation is not included in the simulations. The simulations are carried out with $90^{\circ}_{x}240^{\circ}_{y}90^{\circ}_{x}$ composite pulses and compensation trains (blue), single 180° pulses with compensation trains (green), and $90^{\circ}_{x}240^{\circ}_{y}90^{\circ}_{x}$ composite pulses without compensation trains (red); all pulses were phase cycled using the XY-4 scheme. In general, dispersion profiles are reduced by the application of the compensation trains, with the level of reduction increasing for $90^{\circ}_{x}240^{\circ}_{y}90^{\circ}_{x}$ composite pulses that are of longer duration than their single 180° counterparts. The reduction is more significant for faster exchange process. These effects are included in our fitting routine that simulates the same CPMG element as used experimentally and thus do not introduce errors into the fitted exchange parameters. For dispersion profiles recorded with ν_{CPMG} values > 300 Hz exclusively where there is little difference in the performance of composite vs. single pulses we recommend using single pulses that (i) increase slightly the size of dispersions, as shown here, and that (ii) lead to smaller $R_{2,\text{eff}}(\nu_{\text{CPMG}} = \infty)$ values (Figure S6). Note that the dispersion curves become more similar as the ^{1}H B_1 field used increases, as expected.

References

[1] V. Tugarinov, L. E. Kay, *J. Biomol. NMR* **2004**, *28*, 165–172.

[2] A. K. Schütz, L. E. Kay, *eLife* **2016**, *5*, e20143.

[3] N. K. Goto, K. H. Gardner, G. A. Mueller, R. C. Willis, L. E. Kay, *J. Biomol. NMR* **1999**, *13*, 369–374.

[4] J. R. Huth, C. A. Bewley, B. M. Jackson, A. G. Hinnebusch, G. M. Clore, A. M. Gronenborn, *Protein Sci.* **1997**, *6*, 2359–2364.

[5] D. M. Korzhnev, T. L. Religa, W. Banachewicz, A. R. Fersht, L. E. Kay, *Science* **2010**, *329*, 1312–1316.

[6] R. Sprangers, L. E. Kay, *Nature* **2007**, *445*, 618–622.

[7] A. K. Schütz, E. Rennella, L. E. Kay, *Proc. Natl. Acad. Sci. USA* **2017**, *114*, E6822–E6829.

[8] D. M. Korzhnev, K. Kloiber, V. Kanelis, V. Tugarinov, L. E. Kay, *J. Am. Chem. Soc.* **2004**, *126*, 3964–3973.

[9] P. Lundström, P. Vallurupalli, T. L. Religa, F. W. Dahlquist, L. E. Kay, *J. Biomol. NMR* **2007**, *38*, 79–88.

[10] V. Tugarinov, L. E. Kay, *J. Am. Chem. Soc.* **2007**, *129*, 9514–9521.

[11] T. Yuwen, P. Vallurupalli, L. E. Kay, *Angew. Chem. Int. Ed.* **2016**, *55*, 11490–11494.

[12] F. A. A. Mulder, N. R. Skrynnikov, B. Hon, F. W. Dahlquist, L. E. Kay, *J. Am. Chem. Soc.* **2001**, *123*, 967–975.

[13] M. Tollinger, N. R. Skrynnikov, F. A. A. Mulder, J. D. Forman-Kay, L. E. Kay, *J. Am. Chem. Soc.* **2001**, *123*, 11341–11352.

[14] D. M. Korzhnev, X. Salvatella, M. Vendruscolo, A. A. Di Nardo, A. R. Davidson, C. M. Dobson, L. E. Kay, *Nature* **2004**, *430*, 586–590.

[15] M. H. Levitt, *J. Magn. Reson.* **1982**, *50*, 95–110.

[16] H. Geen, R. Freeman, *J. Magn. Reson.* **1991**, *93*, 93–141.

[17] D. F. Hansen, P. Vallurupalli, L. E. Kay, *J. Phys. Chem. B* **2008**, *112*, 5898–5904.

[18] A. J. Shaka, J. Keeler, T. Frenkiel, R. Freeman, *J. Magn. Reson.* **1983**, *52*, 335–338.

[19] T. Gullion, D. B. Baker, M. S. Conradi, *J. Magn. Reson.* **1990**, *89*, 479–484.

[20] D. Marion, M. Ikura, R. Tschudin, A. Bax, *J. Magn. Reson.* **1989**, *85*, 393–399.

[21] V. Sklenar, M. Piotto, R. Leppik, V. Saudek, *J. Magn. Reson.* **1993**, *102*, 241–245.

[22] J. Cavanagh, W. J. Fairbrother, A. G. Palmer, M. Rance, N. J. Skelton, *Protein NMR Spectroscopy*, Academic Press, London, 2nd ed., **2007**.

[23] J. P. Loria, M. Rance, A. G. Palmer, *J. Am. Chem. Soc.* **1999**, *121*, 2331–2332.

[24] R. Ishima, D. A. Torchia, *J. Biomol. NMR* **2003**, *25*, 243–248.

[25] F. Delaglio, S. Grzesiek, G. W. Vuister, G. Zhu, J. Pfeifer, A. Bax, *J. Biomol. NMR* **1995**, *6*, 277–293.

[26] H. M. McConnell, *J. Chem. Phys.* **1958**, *28*, 430–431.

[27] J. E. Ollerenshaw, V. Tugarinov, L. E. Kay, *Magn. Reson. Chem.* **2003**, *41*, 843–852.

[28] V. Tugarinov, P. M. Hwang, J. E. Ollerenshaw, L. E. Kay, *J. Am. Chem. Soc.* **2003**, *125*, 10420–10428.

[29] A. B. Gopalan, T. Yuwen, L. E. Kay, P. Vallurupalli, *J. Biomol. NMR* **2018**, *72*, 79–91.

[30] D. M. Korzhnev, A. K. Mittermaier, L. E. Kay, *J. Biomol. NMR* **2005**, *31*, 337–342.

[31] V. Tugarinov, L. E. Kay, *J. Phys. Chem. B* **2013**, *117*, 3571–3577.

```
/* 13CH3_1H_SQ_CPMG_lek_800_cp

    This pulse sequence will allow one to perform the following experiment:

    2D 1H/13C to measure exchange using 1H SQ magnetization from methyl groups

           (tau 180 tau)ncyc C 180y C (tau 180 tau)ncyc

    where C refers to compensation 1H 180o pulses that compensate for the fact that
      starting from SQ coherence, different coherences are created during the
      evolution of the pulse

    Assumes that sample is specifically 13CH3 labeled

        1H: O1 on methyl groups (~1.0ppm)
            pwh = p1 1H pw90 @ power level pl1 highest power
            pwh_cp = p15 1H pw90 @ power level pl15 for CPMG pulses

       13C: O2 centre at 20 ppm
            pwc = p2 13C pw90 @ power level pl2 highest power
            power level pl21 is used for 13C decoupling.

    Pulse sequence has the option to use regular 180o 1H pulses or 90x240y90x
      (-Dcomp180_flg); the composite pulses are recommended

    Pulse sequence has the option to begin the CPMG with equal amounts of inphase
      and antiphase (-Dipap_flg) so as to minimize the effects of different
      relaxation between the two that results from Cz. Recommend to use it - there
      is no penalty in terms of extra delays

    Recommend: use -Dipap_flg -Dcomp180_flg -Dwater_flg -Df1180

    This method compensates so that the number of 1H 180os is fixed. Does not
      include any 180o in the reference plane. The alternative is to set -Dref_flg
      that then includes the full number of 1H 180 in the reference plane (gives
      lower R2,eff) - not recommended

    Sequence has option for reburp flag in the center of the CPMG period - not used.

    The sequence uses a fixed time_T2 that is independent of the number of 1H 180o
      pulses

    Sequence uses xy4 based phase cycle as simulations so that this is preferred
      over xy16

    Use ncyc_max = 4*k

*/

prosol relations=<triple>

#include <Avance.incl>
#include <Grad.incl>
#include <Delay.incl>

/***********************/
/*   Define phases     */
/***********************/
#define zero ph=0.0
#define one ph=90.0
#define two ph=180.0
#define three ph=270.0

/***********************/
/*   Define pulses     */
/***********************/
define pulse dly_pg1     /* Messerle purge pulse */
  "dly_pg1=5m"
define pulse dly_pg2     /* Messerle purge pulse */
  "dly_pg2=dly_pg1/1.62"
define pulse pwh
  "pwh=p1"               /* 1H hard pulse at power level p1 (tpwr) */
define pulse pwc
```

```
  "pwc=p2"                /* 13C pulse at power level pl2 (dhpwr) */

define pulse pwh_cp       /* 1H CPMG pulse power level */
  "pwh_cp=p15"

#ifdef water_flg
  define pulse pw_sl1
    "pw_sl1=p14"          /* Eburp1 pulse, ~7000 us */
#endif

#ifdef reb_flg
  define pulse pwh_reb
  "pwh_reb=4.875/(cnst8*bf1/1e6)"   /* REBURP pulse length */
  "spw8=plw15*(pow((p15*2.0/pwh_reb)/0.07981,2))"   /* REBURP power level  */
#endif /*reb_flg*/

/************************/
/*   Define delays      */
/************************/
define delay hscuba       /* length of 1/2 scuba delay */
  "hscuba=30m"
define delay taua
  "taua=d3"               /* d3 = 1/4JHC exactly */

define delay time_T2
  "time_T2=d6"            /* CPMG duration <= 40 ms  */

"in0=inf1/2"
"d11=30m"
"TAU2=0.2u"

/************************/
/*   Define f1180       */
/************************/
#ifdef f1180
  "d0=(in0/2)"
#else
  "d0=(0.2u/2)"
#endif

/************************************/
/* Define parameters related to CPMG */
/************************************/
define delay tauCPMG
define delay tauCPMG1

define list<loopcounter> ncyc_cp=<$VCLIST>

/*******************************************************/
/* Assign cnsts to check validity of parameter ranges */
/*******************************************************/
#ifdef fsat
  "cnst10=plw10"          /* tsatpwr pl10 - set max at 0.00005W */
#endif

#ifdef mess_flg
  "cnst11=plw11"          /* tpwrmess pl11 - set max at 1.0W */
#endif

#ifdef water_flg
  "cnst14=spw14"          /* power level for eburp1 pulse preeceding start of sequenc
e */
#endif

"cnst15=plw15"            /* tpwrcp - power level for 1H CPMG pulses */
"cnst21=plw21"            /* dpwr pl21 - set max at 2.0W */

/*********************/
/* Define CPMG pulses */
/*********************/
#ifdef comp180_flg
#define cpmg_11 (pwh_cp ph12 pwh_cp*2.66667 ph11 pwh_cp ph12):f1
#define cpmg_13 (pwh_cp ph14 pwh_cp*2.66667 ph13 pwh_cp ph14):f1
```

```
#define cpmg_21 (pwh_cp ph22 pwh_cp*2.66667 ph21 pwh_cp ph22):f1
#define cpmg_23 (pwh_cp ph24 pwh_cp*2.66667 ph23 pwh_cp ph24):f1
"cnst51=2.333335"
#else
#define cpmg_11 (pwh_cp*2.0 ph11):f1
#define cpmg_13 (pwh_cp*2.0 ph13):f1
#define cpmg_21 (pwh_cp*2.0 ph21):f1
#define cpmg_23 (pwh_cp*2.0 ph23):f1
"cnst51=1.0"
#endif

#define cpmg_F if "(nsdone+2)%8 < 4" {\n cpmg_11 \n}\n else {\n cpmg_13 \n}
#define cpmg_R if "(nsdone+2)%8 < 4" {\n cpmg_21 \n}\n else {\n cpmg_23 \n}

#ifndef no_compensate
  define loopcounter ncyc_max /* max value of ncyc used */
    "ncyc_max=l8"

  "DELTA8 = pwh_cp*2.0*cnst51*ncyc_max*2.0"
#endif

/************************/
/* Initialize variables */
/************************/
"l1=0"
"l2=0"
"l3=0"
"spoal8=0.5"
"spoff8=0"
"spoal14=1"
"spoff14=0"

aqseq 321

"acqt0=0"
baseopt_echo

1 ze
/*********************************************************************/
/* Check validity of parameters and assign values to some of them */
/*********************************************************************/
#ifdef fsat
  if "cnst10 > 0.00005" {
    2u
    print "error: tpwrmess pl10 too large; < 0.00005W !!!"
    goto HaltAcqu
  }
#endif

#ifdef mess_flg
  if "cnst11 > 1" {
    2u
    print "error: tpwrmess pl11 too large; < 1W !!!"
    goto HaltAcqu
  }
#endif

#ifdef water_flg
  if "cnst14 > 0.01" {
    2u
    print "error: power level for eburp1 pulse is too large; < 0.01W !!!"
    goto HaltAcqu
  }
#endif

  if "cnst15 > 15" {
    2u
    print "error: 1H CPMG power pl15 too large; < 15W !!!"
    goto HaltAcqu
  }

  if "time_T2 > 40.1m" {
    2u
```

```
    print "error: time_T2 too long; < 41ms !!!"
    goto HaltAcqu
  }

#ifndef no_compensate
  if "ncyc_max > 80" {
    2u
    print "error: ncyc_max too large; < 80 !!!"
    goto HaltAcqu
  }

  if "DELTA8 > 10m" {
    2u
    print "error: CPMG pulse duration too long; < 10ms !!!"
    goto HaltAcqu
  }
#endif

  if "cnst21 > 2.0" {
    2u
    print "error: dpwr pl21 too large; < 2.0W !!!"
    goto HaltAcqu
  }

  if "aq > 64m" {
    2u
    print "error: aq is too long; < 64ms !!!"
    goto HaltAcqu
  }

2 d11 do:f2
/************************/
/* Update list pointers */
/************************/
  2u
  "ncyc_cp.idx=l1"
  2u rpp11 rpp12 rpp13 rpp14 rpp21 rpp22 rpp23 rpp24

/***************************************/
/* Continue to check run time variables */
/***************************************/
  "l2 = (trunc(ncyc_cp + 0.3))"
   2u
#ifdef no_compensate
  "l3 = 0"
#else /*no_compensate*/
#ifdef ref_flg
  "l3 = (trunc(ncyc_max - l2 + 0.3))"
#else /*ref_flg*/
  if "l2 > 0 " {
    "l3 = (trunc(ncyc_max - l2 + 0.3))"
  }
  else {
    "l3 = 0"
  }
#endif /*ref_flg*/
#endif /*no_compensate*/

  if "l2 > 80" {
    2u
    print "error: ncyc_cp must be < 81 !!!"
    goto HaltAcqu
  }

  if "l2 > 0" {
    "tauCPMG = (time_T2*0.25)/l2"
#ifdef no_compensate
    "tauCPMG1 = tauCPMG - pwh_cp*cnst51"
#else
    "tauCPMG1 = tauCPMG - (DELTA8*0.25 + 0.2u*l3)/l2"
#endif
  }
  else {
```

```
    "tauCPMG = time_T2*0.25"
    "tauCPMG1 = 2u"
  }

/***********************************/
/* 1H heating compensation period */
/***********************************/
  4u pl15:f1

#if defined(ref_flg) || defined(no_compensate)
  "DELTA = 20u"
#else
  if "l2 == 0" {
    "DELTA = DELTA8 + 20u"
  }
  else {
    "DELTA = 20u"
  }
#endif

  DELTA cw:f1 ph26
  2u do:f1

/*************************************************/
/* Destroy residual 1H magnetization prior to d1 */
/*************************************************/
  20u UNBLKGRAD

  10u fq=cnst1(sfo hz):f1   /* 1H SFO1 @ tof(water) */
  4u pl1:f1              /* power pl1 for 1H pulses */
  (pwh ph26):f1

  2u
  p50:gp0*0.5
  d16

  (pwh ph27):f1

  2u
  p50:gp0
  d16

  4u BLKGRAD

/******************/
/* Messerle purge */
/******************/
#ifdef mess_flg
  4u pl11:f1
  (dly_pg1 ph26):f1
  2u
  (dly_pg2 ph27):f1
#endif

/*****************/
/* Presaturation */
/*****************/
#ifdef fsat
  4u pl10:f1
  d1 cw:f1 ph26
  2u do:f1
  4u pl1:f1
#ifdef fscuba
  hscuba
  (pwh ph26 pwh*2.0 ph27 pwh ph26):f1
  hscuba
#endif /*fscuba*/
#else  /*fsat*/
  4u pl1:f1
  d1
#endif /*fsat*/
  20u UNBLKGRAD
```

```
/*************************/
/* Water selective Eburp1 */
/*************************/
#ifdef water_flg
  2u
  (pw_sl1:sp14 ph26):f1
  2u

  2u
  p50:gp0
  d16
#endif

/***************************************/
/* Destroy 13C equlibrium magnetization */
/***************************************/
  4u pl2:f2
  (pwc ph26):f2

  2u
  p50:gp0
  d16

/*************************/
/* This is the real start */
/*************************/
  10u fq=0(sfo hz):f1
  4u pl1:f1

  (pwh ph26):f1

  2u
  p51:gp1
  d16

  "DELTA = taua*2.0 - 2u - p51 - d16 - pwh*2.0/PI"
  DELTA

/*******************/
/*    t1 period    */
/*******************/
  (pwc ph1):f2

  "TAU1=larger(d0-pwh*2.0-pwc*2.0/PI,TAU2)"
  TAU1

  (pwh ph26 pwh*2.0 ph27 pwh ph26):f1

  TAU1

  (pwc ph26):f2

/************************************************/
/* Option to create 50%/50% IP/AP prior to CPMG */
/************************************************/
#ifdef ipap_flg
  if "nsdone%4 < 2" {
    "DELTA = taua + 4u"
    DELTA

    (pwh ph26 pwh*2.0 ph27 pwh ph26):f1
  }
  else {
    "DELTA = taua - 4u"
    DELTA
  }
#else
  4u
  (pwh ph26 pwh*2.0 ph27 pwh ph26):f1
#endif
  4u pl15:f1

/*********************************/
```

```
/* The first half of CPMG period */
/*******************************/
  if "l2 > 0" {
3   tauCPMG1
    cpmg_F
    tauCPMG1 ipp11 ipp12 ipp13 ipp14 ipp21 ipp22 ipp23 ipp24
    lo to 3 times l2

  }

  if "l3 > 0" {
4   0.2u
    cpmg_F
    0.2u ipp11 ipp12 ipp13 ipp14 ipp21 ipp22 ipp23 ipp24
    lo to 4 times l3
  }

/*****************************/
/* The central 180o 1H pulse */
/*****************************/
#ifdef reb_flg
  4u
  (pwh_reb:sp8 ph2):f1
  4u pl15:f1
#else /*reb_flg*/
  (pwh_cp*2.0 ph2):f1
#endif /*reb_flg*/

/*********************************/
/* The second half of CPMG period */
/*********************************/
  if "l3 > 0" {
5   0.2u dpp11 dpp12 dpp13 dpp14 dpp21 dpp22 dpp23 dpp24
    cpmg_R
    0.2u
    lo to 5 times l3
  }

  if "l2 > 0" {
6   tauCPMG1 dpp11 dpp12 dpp13 dpp14 dpp21 dpp22 dpp23 dpp24
    cpmg_R
    tauCPMG1
    lo to 6 times l2
  }

/***********************/
/* C->H back transfer */
/***********************/
#ifdef ipap_flg
  if "nsdone%4 >= 2" {
    4u pl1:f1
    (pwh ph26 pwh*2.0 ph29 pwh ph26):f1
    4u
  }
#endif

#ifdef ipap_flg
  "DELTA = taua - 2u - p51 - d16 - 4u - 4u - de"
#else
  "DELTA = taua*2.0 - 2u - p51 - d16 - 4u - 4u - de"
#endif
  DELTA

  2u
  p51:gp1
  d16

/*************************************************************/
/* Option for 3-9-19 Watergate for better water suppression */
/*************************************************************/
#ifdef wgate_flg
  4u pl1:f1
  "DELTA = 4u + 4u + de + 4u + de"
```

```
  DELTA

  2u
  p52:gp2
  d17

  (pwh*0.231 ph27):f1
  d19*2.0
  (pwh*0.692 ph29):f1
  d19*2.0
  (pwh*1.462 ph27):f1
  d19*2.0
  (pwh*1.462 ph27):f1
  d19*2.0
  (pwh*0.692 ph29):f1
  d19*2.0
  (pwh*0.231 ph27):f1

  2u
  p52:gp2
  d17
#endif

  4u BLKGRAD
  4u pl21:f2             /* lower power for 13C decoupling */

/*********************************/
/* Signal detection and looping */
/*********************************/
  go=2 ph31 cpds2:f2
  d11 do:f2 mc #0 to 2
    F2QF(calclc(l1, 1))
    F1PH(calph(ph1, +90), caldel(d0, +in0) & calph(ph1, +180) & calph(ph31, +180))

HaltAcqu, 1m
exit

ph0=1
ph1=0 2
ph2=1 1 3 3 1 1 3 3 3 3 1 1 3 3 1 1
ph11=0 1 0 1
ph12=ph11-ph0
ph13=1 0 1 0
ph14=ph13-ph0
ph21=0 3 0 3
ph22=ph21+ph0
ph23=3 0 3 0
ph24=ph23+ph0
ph26=0
ph27=1
ph28=2
ph29=3
ph31=0 2

;d1: Repetition delay D1
;d3: taua - set to 1/4JHC = 2.0 ms
;d6: time_T2 CPMG duration <= 40ms
;d11: delay for disk i/o, 30ms
;d16: gradient recovery delay, 200us
;d17: gradient recovery delay for 3-9-19 watergate, 200us
;d19: delay for binomial water suppression, ~1/(4*|cnst1|)
;pl1: tpwr - power level for pwh
;pl2: dhpwr - power level for 13C pulse pwc (p2)
;pl10: tsatpwr - power level for presat
;pl11: tpwrmess - power level for Messerle purge
;pl15: power level for 1H CPMG pulses pwh_cp
;pl21: dpwr - power level for  13C decoupling cpd2
;sp14: power level for eburp1 pulse
;spnam8: Reburp.1000
;spnam14: eburp1 pulse on water
;p1: pwh
;p2: pwc
;p14: eburp1 pulse width, typically 7000us
```

```
;p15: 1H pw for CPMG pulses
;p50: gradient pulse 50                                  [1000 usec]
;p51: gradient pulse 51                                  [500 usec]
;p52: gradient pulse 52                                  [800 usec]
;cpdprg2: 13C decoupling program during t2 [waltz16]
;pcpd2: 13C pulse width for 13C decoupling
;cnst1: offset of water from methyls (Hz)
;cnst8: methyl H excitation bandwidth (ppm)
;vclist: variable counter list for ncyc_cp
;l8: ncyc_max (MUST BE SET PROPERLY!)
;delta8: total duration of 1H CPMG pulses
;inf1: 1/SW(X) = 2*DW(X)
;in0: 1/(2*SW(x))=DW(X)
;nd0: 2
;ns: 4*n
;FnMODE: States in F1
;FnMODE: QF in F2

;for z-only gradients:
;gpz0: 20%
;gpz1: 30%
;gpy2: 0% (Z-gradient) or 80% (XYZ-gradient)
;gpz2: 80% (Z-gradient) or 0% (XYZ-gradient)

;use gradient files:
;gpnam0: SMSQ10.32
;gpnam1: SMSQ10.32
;gpnam2: SMSQ10.32

;zgoptns: Dfsat, Dmess_flg, Dfscuba, Dwater_flg, Dwgate_flg, Df1180, Dcomp180_flg, D
ipap_flg, Dreb_flg, Dref_flg, Dno_compensate
```